Engineering and Technology Journal
Journal homepage: https://etj.uotechnology.edu.iq

Improving Fatigue Corrosion Resistance of Turbine Blades Using Laser Processing

Zaman A. Abdulwahab*, **Sami I. Jafar , Sami A. Ajeel**

Production & Metallurgy Engineering Dept., University of Technology-Iraq, Alsina'a street, 10066 Baghdad, Iraq.
*Corresponding author Email: pme.19.46@grad.uotechnology.edu.iq

HIGHLIGHTS

- Laser modification was performed on the blades of a turbine.
- Powders of Inconel 600 were deposited on the steel substrate.
- Wear resistance was attributable to the surface hardening layer and wear debris layer.
- The laser-affected region is divided into oxide, severe deformed, and moderate zone.
- The microstructure of steels after laser processing is greatly refined with equiaxed grains.

ARTICLE INFO

Handling editor: Mustafa H. Al-Furaiji

Keywords:
Turbine blades
Fatigue corrosion
Laser cladding process
nanoparticle coating
Inconel 600

ABSTRACT

The present paper investigates the nanomaterial coatings effect on turbine blades by laser processing. The present paper explores the impact of laser cladding parameters on the corrosion behavior of the resulting surface. Powders of Inconel 600 were deposited on the steel substrate. The surface can be thought of as the most important part of every engineering component. Unlike the rest of the component's volume, the surface is exposed to wear and becomes the place where most cracks form and corrosion initiates. Corrosion is one of the most harmful problems affecting turbine blades. In the current investigation, coating nanomaterials, namely Inconel 600, have been used to resist corrosion. The specimens of tests have been obtained from the part of the turbine blades in Al-Doura Station, located south of Baghdad. These specimens are separated into two groups: The 1st group is received specimens, and the 2nd group is with nanoparticle coating, including Inconel 600 coating applied by laser cladding. The procedure of cladding was implemented utilizing the following parameters :(11 j) pulse energy, (6 Ms.) pulse width, (12 Hz) pulse frequency, (132 W) laser average power, and (1.83 KW) laser peak power. The results show that the microstructure of steels after laser processing is greatly refined with equiaxed grains and highly homogeneous as compared with those of steels before laser treatment, resulting in a significant improvement in strength, toughness, and fatigue corrosion.

1. Introduction

Various methods have been used to avoid corrosion fatigue of the turbine blades [1]. The main objective work of turbine blades is converting the steam's linear motion at high pressure and temperature into rotation motion. The superheated steam enters a turbine, where the stored energy is utilized to move the turbine shaft, generating electricity [2] using crack morphology, fractography, and composition analysis to determine the causes of blade failure due to environment-aided fatigue fracture. Fatigue fracture initiation is linked to the salient of blades because of the high-stress concentration. Increased tempering temperature in modified treatment and high-frequency hardening was suggested to reduce blade cracking [3]. Corrosion fatigue failures of steam turbine blades have been a major problem for more than 30 years across the globe. SEM findings of intergranular fracture and fatigue failure under lower stress than design stress prompted the subject of corrosion fatigue failure in the steam turbine blade [4]. The chemical composition and heat treatment influence martensitic stainless steel's mechanical qualities and corrosion resistance. Steel was treated with austenite (austenitizing), followed by chilling or quenching (to turn austenite into martensite), and then treated by tempering (to precipitate carbides). Concerning this metal, the quantity of carbide may impact its mechanical qualities and corrosion resistance. In addition, Austenite retention may affect wear resistance, fatigue life, and ductility [5]. Surface modification technology has grown in relevance as laser applications in automobiles, airplanes, ships, and other heavy sectors have expanded rapidly. It has much room to expand as a wear-resistant coating for hard materials. Aside

http://doi.org/10.30684/etj.2022.134330.1235
Received 06 August 2022; Accepted 02 October 2022; Available online 17 November 2022
2412-0758/University of Technology-Iraq, Baghdad, Iraq

from this, current developments in hard-facing engine valve seats, turbine blade shroud interlocks, and the leading edge of steam turbine blades with controlled dilution have attracted great attention [6].

The authors have investigated laser cladding since 2001 to deposit a high-quality and erosion-resistant barrier on the leading edge of LP blades. The research established the viability of in situ turbine blade replacement at a power plant using a fiber-delivered diode laser and a robot in experiments. As a result, 340 LP blades were repaired by Hardwar Pty Ltd, a business founded in late 2005 to commercialize this technology [2]. As one of the most important steam turbine parts, the blade is critical to its safe and efficient functioning. Wind energy may be converted into mechanical energy via a blade—especially the blades in the last step. Small water droplets are ejected at the end of the blades and burst with high-speed centrifugal action when the steam condenses into water droplets. After a lengthy period of use, blades will develop fatigue fractures at the ends. According to the statistics, several turbine-generator accidents were caused by blade failure [7].

Another major source of steam turbine unexpected outages is rotor blade failure, which is a typical occurrence. A turbine blade breaks during operation poses a safety hazard since a catastrophic failure might follow. Injuries and death may result from a steam turbine's catastrophic collapse of any size, regardless of the turbine's size [8]. Typically, the turbine is destroyed, causing the facility to be shut down for a long time. – There are significant operating revenue losses for the facility in this instance. Repairing a turbine is expensive and takes a long time. Rotor blade dependability is critical to a steam turbine's safe and effective operation [9].

Corrosion fatigue failures in steam turbine blades and cargo oil tanks were used as case studies. On 12 Cr stainless steel steam turbine blades and high-strength steel ship hulls, the mechanisms of corrosion fatigue, affecting factors, and countermeasures have been briefly outlined, mostly from the author and his colleagues' experimental data [10]. There are dangerous contaminants in the steam turbine environment, not just pure steam. This includes dissolution from boiler feedwater or saturated steam mist and scale oxidation and dissolution from the superheater. Resonance fatigue failure of steam turbine moving blades may be readily seen on the fracture surface by the naked eye.

In contrast, corrosion fatigue failure of steam turbine blades is characterized by the following events. First, the earliest corrosion pits may often be seen if the region is well maintained following a failure. As a second example, several micro-cracks are close to corrosion pits [11].

Nanomaterials have a significant impact on both passive and active corrosion-prevention coatings. There are various ways to characterize nanocoatings, such as a coating with a nanoscale thickness, a coating with nanoscale particles in the matrix, or a coating with nanoscale grains or phases. Since the inception of thin-film coatings, a considerable amount of time has elapsed. Nanostructured coatings have grain sizes of 100 nm, whereas nanocomposite coatings have grain sizes below 100 nm [12]. Soil–gel, magnetron sputtering, and electro-spark deposition are vacuum-based procedures. Laser beam surface treatment and high velocity oxy-fuel thermal spray are examples of surface treatments. Higher wear, erosion, high-temperature oxidation, and corrosion resistance are only some of the desired enhancements [13]. Incorporating nanomaterials is reported to fill gaps, stop water and air ingress, and fix minute faults, resulting in more effective passive defenses. Research using nano clay-based composite coatings in vehicle parts has sparked worldwide interest [14]. The use of nanotechnology in the metal/inherent alloy's corrosion resistance and performance might be enhanced by obtaining the necessary finely crystalline microstructure (e.g., nano crystallization). It also may be obtained by altering its chemical composition at the nanometric scale (e.g., production of copper nanoparticles at steel grain boundaries) and by creating coatings and inhibitors with specific characteristics. A crucial example of a nanotechnological technique in manufacturing corrosion-resistant alloys is high-performance steel production with a fine-grain structure or the process of manufacturing self-organization of strengthening nanophases (carbides, nitrides, carbonitrides, intermetal ides). With nanotechnology, corrosive conditions may also be reduced by altering the metal/corrosive electrolyte contact by utilizing metallic and non-metallic coating (e.g., forming nanocomposite coatings on steel) [15]. A nanomaterial has a characteristic size of at least 1 nm. Materials and material systems may have superior qualities when their properties are extended to the nanoscale or scaled up from larger-sized systems. Both of these criteria apply to coatings with nanometer-sized components. Our current knowledge of materials can no longer explain the features of nanostructured materials. Nanostructured materials, according to the researcher [16], act differently from conventional materials for three reasons:

1) surface-volume ratios of more than one;
2) with relation to the size
3) quantum physics consequences.

Corrosion and reactivity of nanostructured materials are thought to be significantly influenced by these two variables (changes in energy level owing to quantum effect and grain size at the nanometer scale) [17].

The viability of in situ turbine blade replacement was established using higher-strength materials or improving the microstructure by conducting heat treatments to obtain fine grains with high strength. It is also possible to use coating with nanoparticles of high-strength metals or ceramic materials with high corrosion resistance and strength. Due to scientific and technological progress and the discovery of lasers with different energies, this technology was introduced to re-melt the surface microstructure with laser treatment. The current research aims to use this new technology that provides high and focused energies in laser cladding the micro-structures of the surface layers and cooling them to obtain microstructures that are resistant to corrosion and have high strength and toughness.

2. Experiments

2.1 Materials

St-52 steel sheet with a thickness of 2 mm and a deposit area of 30 x 90 cm was employed in the present investigation. Table 1 shows the stated chemical compositions from the manufacturers determined by the PMI-master pro (robust, transportable optical emission spectrometers).

Table 1: Chemical composition of St.52

Element wt.%	**C**	**Fe**	**Mn**	**Cr**	**Ni**	**Mo**	**AL**	**Si**
Measured (wt%)	0.204	85.5	0.540	12.8	0.355	0.0782	0.0210	0.342
Element (wt%)	Cu	Co	Ti	V	Pb	W		Nb
Measured (wt%)	0.191	0.0298	0.0040	0.0164	< 0.0150	< 0.0400		0.0036

2.2 Preparation of Samples

2.2.1 Preparation of samples for experimental procedures

Figure 1 shows the steam turbine blades from AL- Doura's station and Figure 2 shows the steam turbine blades after cutting; a portion of a steam turbine blade is cut into a 30 mm x 90 mm rectangle with a 2mm thickness for use in the electrochemical testing. With a Grinder and Polisher MoPao 160E. A rotating disk with abrasive materials ranging from 180, 320, 500, 800, 1000, and 2000 grits is used to grind the specimen material wished with water. These different degrees of grits are necessary to utilize SiC sheets with varying smoothness. Then, specimens are polished with alumina paste to obtain mirror surfaces. Nital solution (a mixture of 98 percent ethanol and 2 percent HNO3) is used for Etching turbine blade specimens. An air drier is used to dry the specimen after being submerged in the solution for around 15 seconds.

Figure 1: Steam turbine blades

Figure 2: The St.52 blades of the steam turbine, after cutting

2.3 Laser Process

Laser processing is a laser surfacing procedure where the goal is to cover a specific area of the substrate with better material, resulting in a fusion connection between the two with minimum mixing (dilution) of the clad by the substrate. A laser system with a Laser Peak Power of 1.83 KW and a Pulse Energy of 11 Joule was used to apply cladding to all specimens at the INLC (Iranian national laser center).

2.4 Energy Dispersive Spectroscopy (EDS) and Scanning Electron Microscopy (S.E.M.)

EDX is the most often used chemical analysis instrument in failure analysis, followed by Energy Dispersive Spectroscopy (EDS). It comes with a slew of noteworthy features. Every failure analysis laboratory has an SEM (Scanning Electron Microscope). The whole process of analysis is completed in a matter of minutes. The spectra are straightforward to decipher.

The resolution of the spatial data is enough. However, as an analytical tool, it has significant drawbacks as well. First, the sampling volume is restricted to concentrations of 0.1 percent or less. As a second drawback, the specimen's volume is excessive since semiconductor thin films and deep submicron particles are so thin. In addition, it only delivers atomic information rather than molecular information [18].

After the laser surface alloying process, an EDS device was employed to determine the surface chemical content. This equipment is often coupled to a scanning electron microscope (SEM) [19].

Magnification may be as high as 100000X using this device. At high and low pressure, the deception resolution is variable. Cams can type MV-2300 produced in the Czech Republic as used for this test at the AL-Razi Metallurgical Research Center in Tehran-Iran.

2.5 Fatigue Corrosion Test

Figure 3 shows the corrosion fatigue device; researchers from the university's production engineering and metallurgy department have measured sample corrosion. Air and solution after laser cladding are two separate groups of experiments.

A model of the steam environment in its final stage might be used to estimate the corrosion rate of steam turbine blades. The same approach was employed at Al-Doura's power plants (steam distillate water). The solution vapor had a temperature of 100 degrees Celsius and a velocity of 3 milliliters per second.

The current research is to design and manufacture a "reciprocating bending stress test machine" that is easy, safe to use, and more accurate than others. The Avery Dennison Type 7305 Frequency Bending Fatigue Tester was developed, taking into account the basic concepts of technical theory and combining the load variables and ambient conditions. This invention generally depends on simulating the ambient conditions that can be controlled (the type of medium is liquid or vapor) and the value of the reciprocating force with which the fatigue device works by changing the bending angle. Filterable, which makes it easy to read the number of cycles directly. The load cell that acts as a stress function changes over time and determines the time of crack formation, which grows until the fracture occurs. Also, the applied effort with which the crack growth begins can be monitored through the display screen to overcome the determining difficulty. The results can be extracted in the form of curves represented by the number of frequencies and effort.

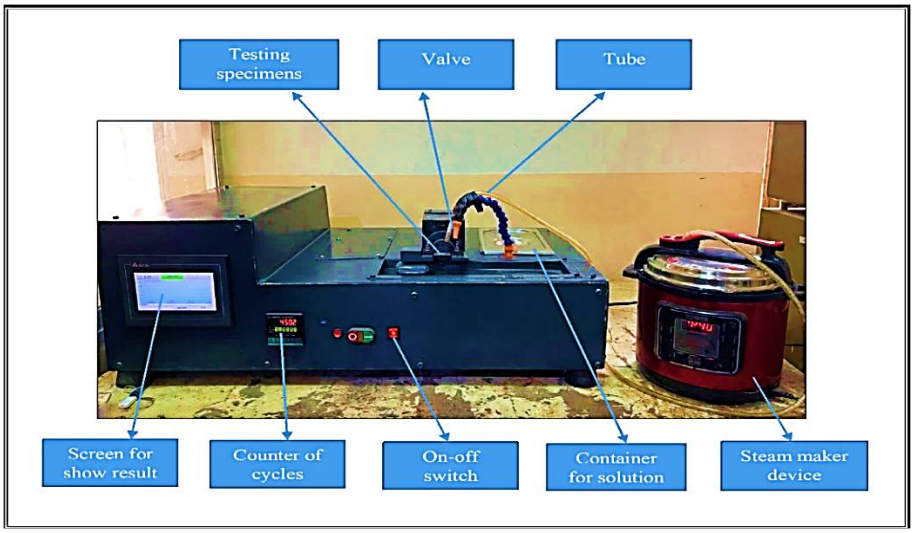

Figure 3: The Device of Fatigue Corrosion

The machine is driven by an electric motor with a speed of 1500 rpm. , movement is transmitted to the unbalanced turntable using two pulleys and a conveyor belt. The torque is generated in the sample under test, and the load value is controlled by changing the angle of the unbalanced rotating disc. Tests can be performed on standard Avery Dennison Type 7305 specimens. The tests can be applied to metallic or non-metallic materials, and the frequency amplitude is constant over time. The rotational effort is measured with a load dynamometer with an automatic mechanism to adjust the load force applied during testing. This not only added mechanical complications to the device but also controlled the test conditions.

3. Results and Discussion

3.1 SEM Examination

Figure 4 shows the scanning electron microscopy results for steam turbine blades. The sample's particle dispersion and surface topography were examined using an SEM. Before corrosion, steam turbine blades have a ferrite and perlite microstructure, as seen in Figure 4a. Steam turbine blades have a microstructure composed of white ferrite and black perlite bolls.

Figure 4b shows dry fatigue begins as cracks take hold of the specimen's surface due to the blade's rotation. As seen in Figure 4c, liquid fatigue occurs on the specimen's surface. There are several cracks in specimens due to fatigue corrosion, as seen in this image. In contrast, Figure 4d depicts the specimen surface after laser cladding, in which the specimen comprises two layers. The first layer was clad alloy and the second layer was substrate. More dilution and lower hardness magnitude are associated with longer interaction durations with coarse structure and longer contact periods with shorter contact periods.

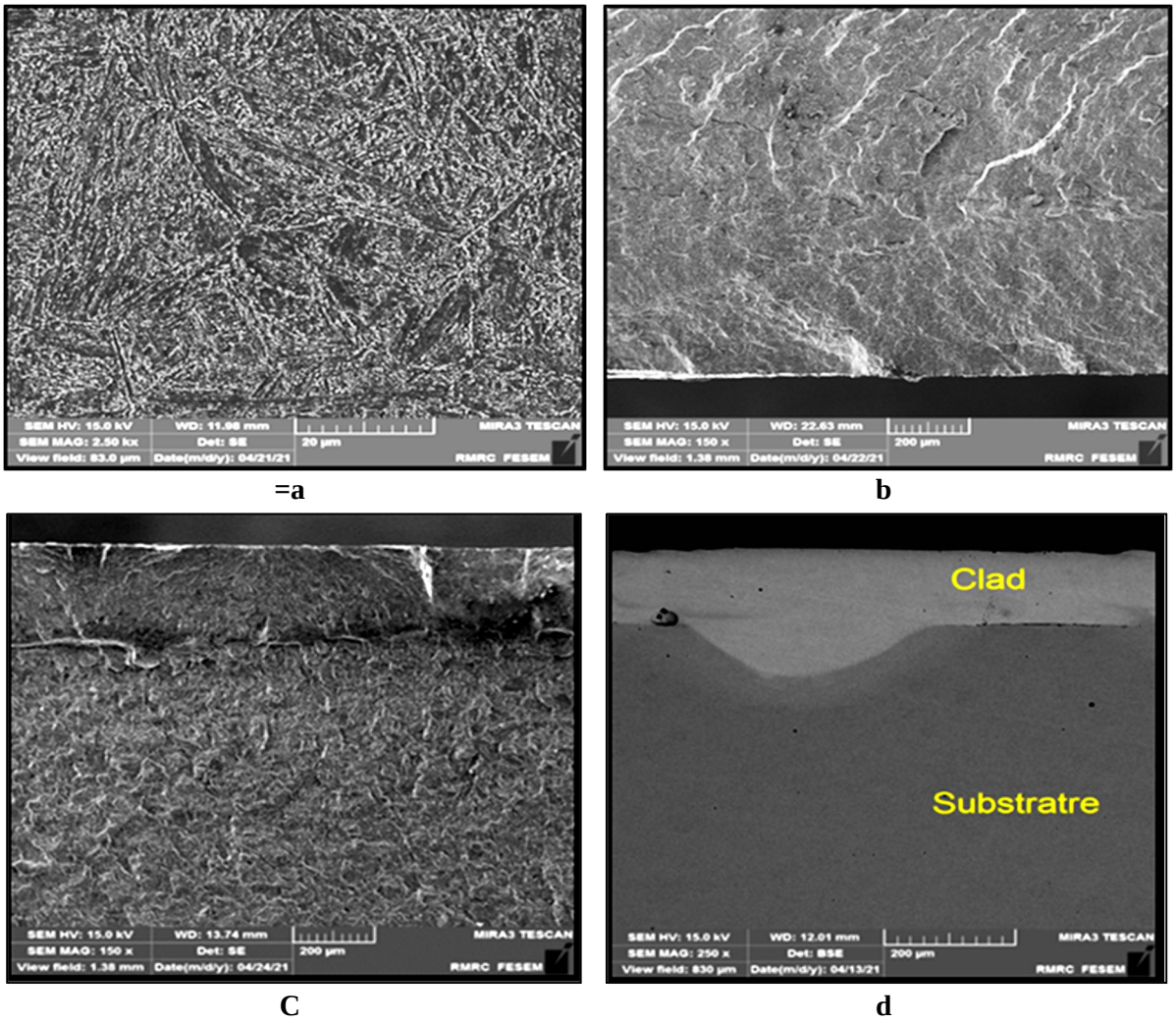

Figure 4: Scanning Electrons Microscope for st.52**a.** Scan Electrons Microscope for st.52, **b**. Scan Electrons Microscope for st.52 after fatigue in air. **c.** Scan Electrons Microscope for st.52 after fatigue corrosion in solution. **d.** Scan Electrons Microscope for st.52 after laser cladding

3.2 Energy Dispersive Spectroscopy (EDS) Results

Energy dispersive spectroscopy was used to conduct the alloys' element analysis, and it was utilized for computing the elements' contents in the tested specimen as a function of weight%. From Table (2), it can be observed that nickel represents the largest percentage by weight in the examined sample at about 72.47%, chromium at about 15.92%, and iron at 11.12%. On the other hand, silicon represents 0.49% of the sample's total weight after A cladding, representing the smallest percentage. The EDS Test for the sample after A cladding is shown in Figure 5.

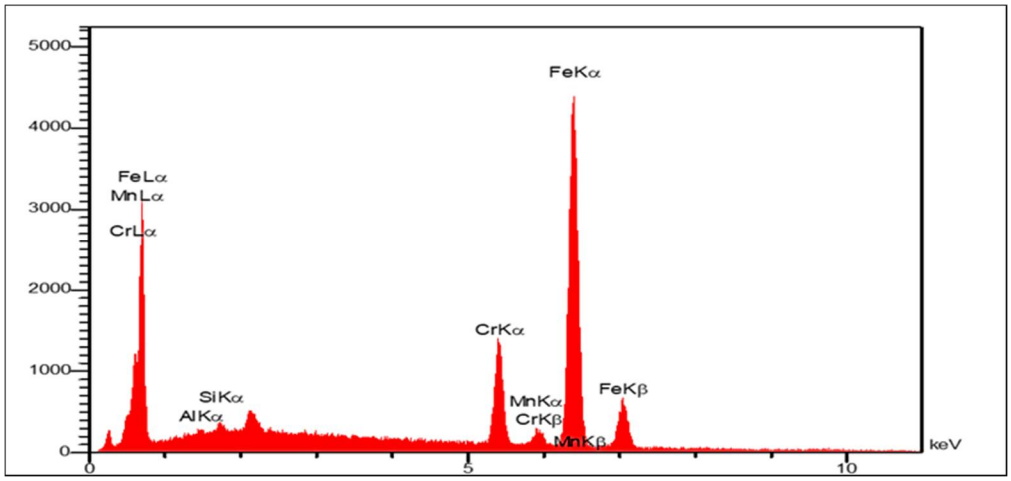

Figure 5: EDS Test for sample after A cladding

Table 2: Quantitative Results for EDS Test Composition sample after A cladding

Elt	line	Int	Error	k	kr	W%	A%	ZAF		OX%	PK/Bg	Class	LConf	HConf	Cat#
Si	Ka	11.0	0.4249	0.0029	0.0029	0.49	0.98	0.6063	Formula	0.00	2.31	B	0.45	0.52	0.00
Cr	Ka	192.1	0.8907	0.1678	0.1690	15.92	17.42	1.0617		0.00	12.15	A	15.62	16.22	0.00
Fe	Ka	96.3	0.8907	0.1213	0.1221	11.12	11.34	1.0979		0.00	8.34	A	10.83	11.42	0.00
Ni	Ka	360.2	0.8907	0.7080	0.7130	72.47	70.26	0.9838		0.00	31.59	A	71.49	73.46	0.00
				1.000	1.007	100.0	100.0			0.00					0.00

From Table 3, it can be observed that Iron represents the largest percentage by weight in the examined sample at about 86%, chromium at about 13.17%, manganese at 0.4 %, and silicon at 0.33%. On the other hand, aluminum represents the lowest weight percentage, with only 0.09 % of the total weight of the specimens after B cladding, as shown in Figure 6.

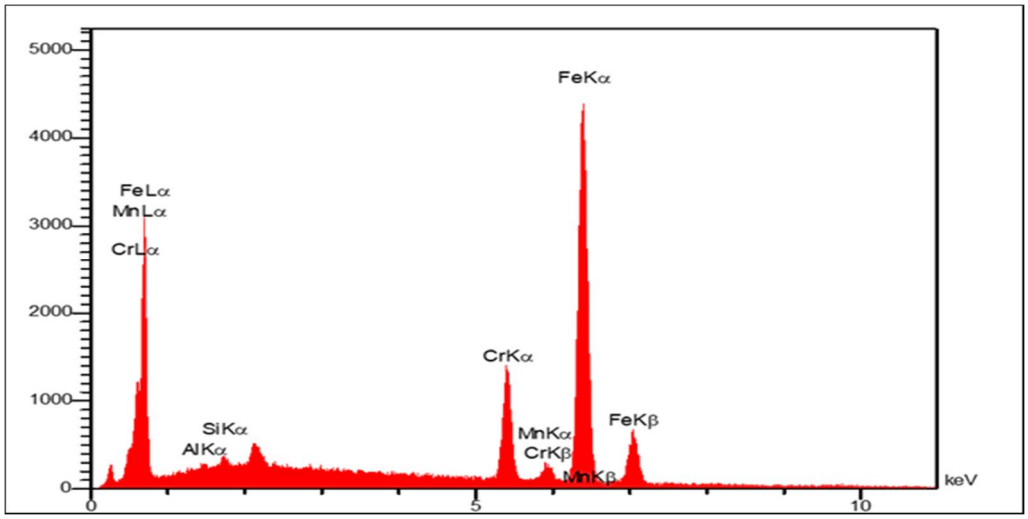

Figure 6: EDS Test for sample after B cladding

Table 3: EDS Test Composition sample after B cladding

Elt	Line	Int	Error	K	Kr	W%	A%	ZAF		OX %	Pk/Bg	Class	LConf	HConf	Cat %
Al	Ka	4.1	0.7998	0.0004	0.0004	0.09	0.18	0.5137	Formula	0.00	2.08	B	0.07	0.10	0.00
Si	Ka	19.6	0.7998	0.0022	0.0022	0.33	0.65	0.6687		0.00	2.31	B	0.31	0.36	0.00
Cr	Ka	417.8	0.8074	0.1543	0.1558	13.17	13.95	1.1829		0.00	12.04	A	12.97	13.38	0.00
Mn	Ka	9.1	0.8074	0.0040	0.0040	0.40	0.40	1.0110		0.00	3.65	B	0.36	0.44	0.00
Fe	Ka	1577.0	0.8074	0.8391	0.8475	86.01	84.82	0.9854		0.00	48.38	A	85.33	86.69	0.00
				1.0000	1.0101	100	100			0.00					0.00

3.3 Corrosion Behavior

Figure 7 shows the fatigue corrosion in air, and Figure 8 shows the fatigue corrosion in solution. The air sample had 46427 cycles of fatigue corrosion, while the solution sample had 33452 cycles of fatigue corrosion. The cycle count is calculated using a corrosion fatigue device.

After laser cladding, the fatigue resistance of the specimens in the air was greater than the specimens in the solution because the specimens in the air needed more cycles before failure.

Stellite 6 clad material's surface degraded following Nair and Khan [20]while considering various powder feed rates. In contrast to the other two situations, the clad tracks are visible at lower powder feed rates. A corroded surface reflects sulfur's influence, and the material has entirely deteriorated, exposing the cladding tracks. The quality of cladding has improved with the growth in cladding powder. At a powder feed rate of 0.15 g/min, the bonding of the clad structure was shown to be better, and the corroded surface in the spheroids was discovered to be caused by partial carbides in form. To support this, the surface viewed under an electron microscope at the highest powder feed rate has distinct dendrites fused with reduced corrosion impact. The specimen test is carried out using an energy dispersive spectroscopy (EDS) examination to validate carbides' existence on the clad surface.

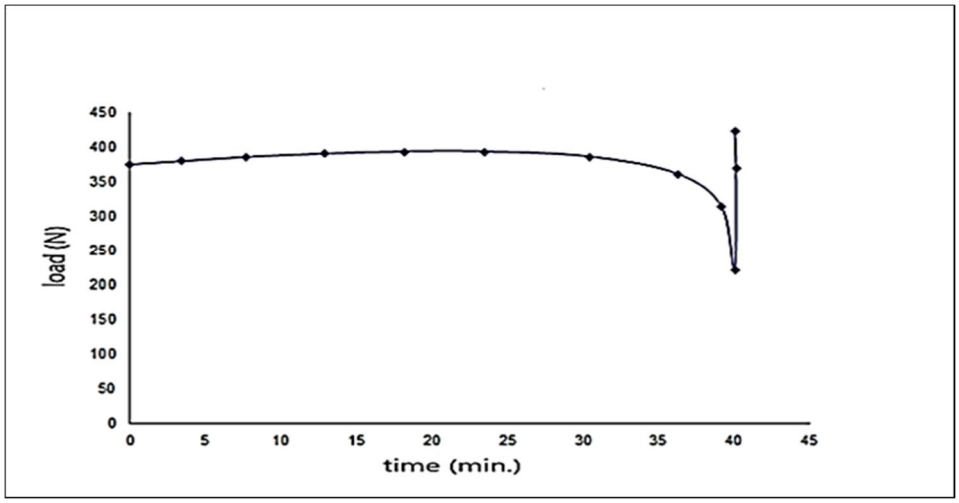

Figure 7: Fatigue specimen in the air

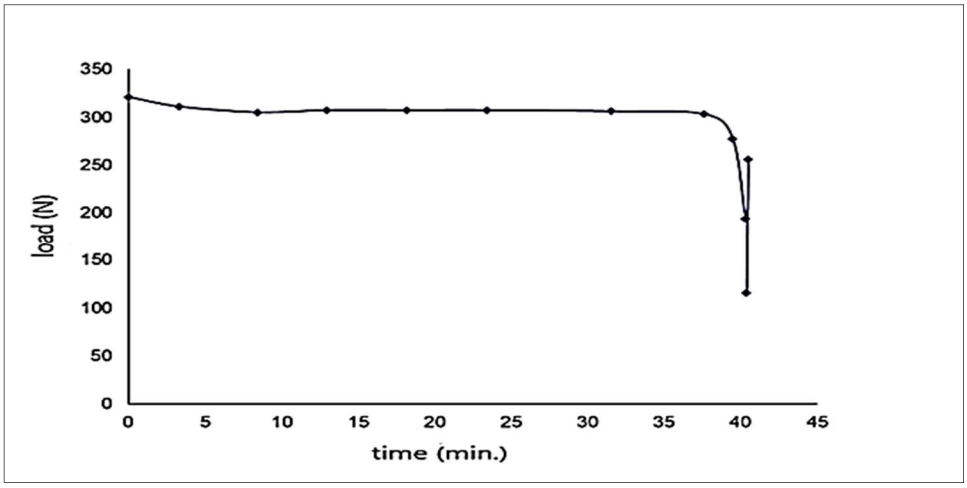

Figure 8: Fatigue corrosion of specimen in the solution

Figure 9 shows the fatigue specimen in the air after the laser cladding, and Figure 10 shows the fatigue corrosion of the specimen in the solution after the laser cladding process. The oxidation layer was removed from the specimens using emery paper before cladding. All samples have been coated using Inconel 600 alloys and a laser system with a peak power of 1.83 KW and pulse energy of 11 Joules. There were (55774) fatigue cycles in air and (24450) fatigue cycles in solution for the specimens that had been laser clad. Figures 9 and 10 demonstrate the effect of laser cladding on fatigue corrosion in steam turbine blades.

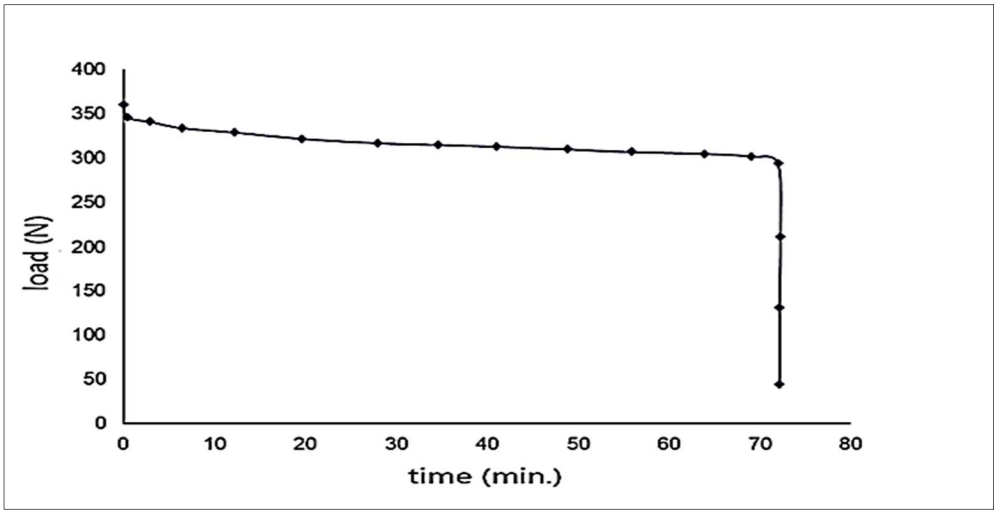

Figure 9: Fatigue specimen in the air after the laser cladding process

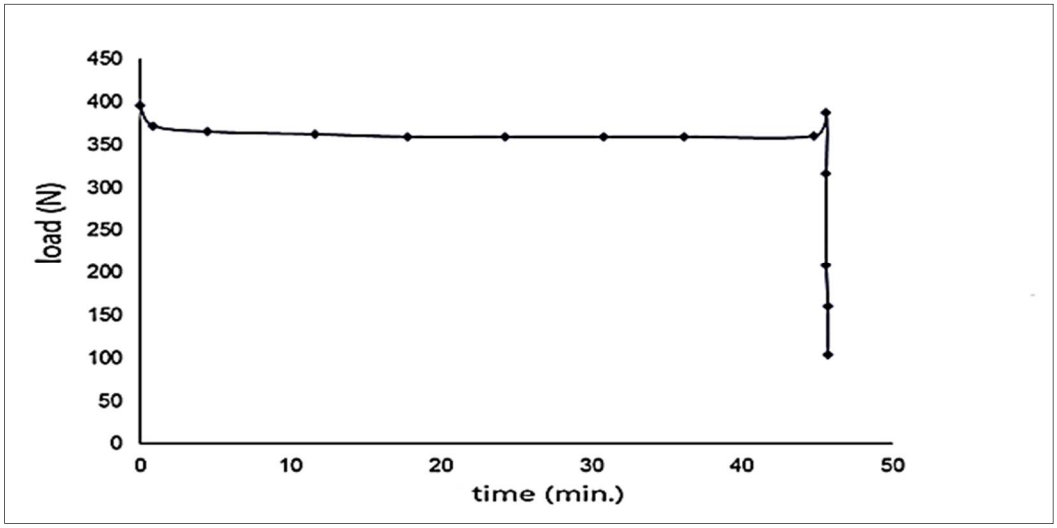

Figure 10: Fatigue corrosion of specimen in the solution after the laser cladding process

Because samples in the air need more fatigue cycles and time to failure, those in solution following laser cladding showed a greater fatigue resistance.Soylu [21] observed that the welding gives higher strength than the original metal, and the sample after cladding behaves similarly

Figure 11 compares fatigue specimens in and after the laser cladding process. Figure 12 compares the fatigue specimen, the fatigue specimen in the air after the laser cladding process, and the fatigue corrosion specimen in solution to the laser cladding process. The fatigue limit (also called the endurance limit) is the stress level below which fatigue failure does not occur. This limit exists only for some ferrous (iron-based) and titanium alloys. Hence, the fatigue limit was high with many cycles [22].

It is clear from Figures 11 and 12 that there is little difference between fatigue specimens shot into the air before and after the cladding was applied by laser. However, the specimens' resistance to fatigue in the air was greater than that of the specimens in solution since the specimens in the air need more fatigue cycles and time before they fail.

Depending on Walker et al. [23], the compressive residual stresses (300 MPa at the surface) brought on by the laser cladding process had a considerable positive impact on the "as-clad" situation, resulting in a decreased fracture development rate and a longer lifespan. For the study, a semi-circular defect with a depth of 47 m that matched the fractography data for Sample 6 was utilized as the beginning crack size. Life was under-predicted by roughly 47% in this instance, but the correlation with the quantitative fractography (QF) data was satisfactory.

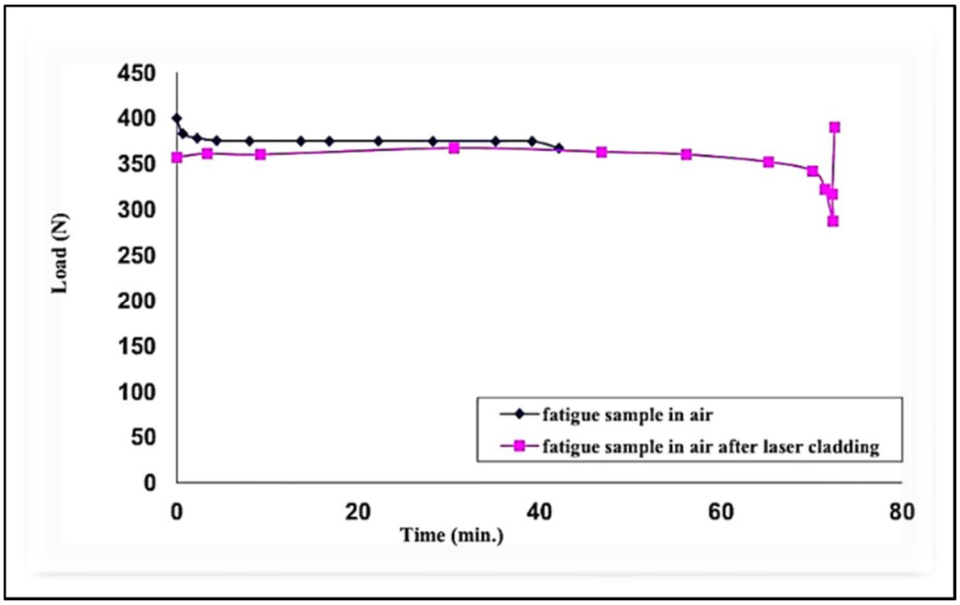

Figure 11: Fatigue specimen in the air and fatigue specimen after the laser cladding process

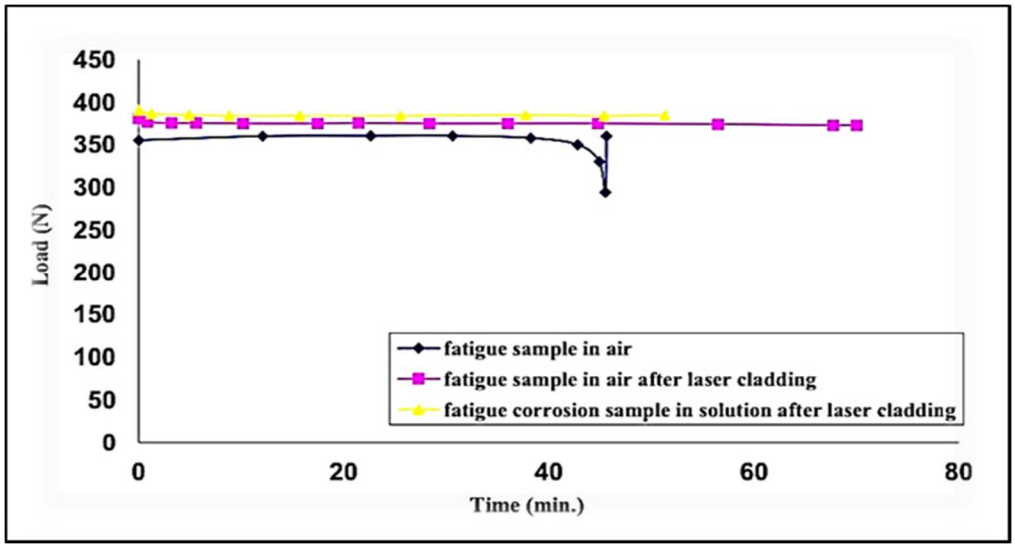

Figure 12: Fatigue specimen in the air, fatigue specimen in the air after the laser cladding process, and fatigue corrosion specimen in solution after the laser cladding process

4. Conclusion

1) In the fatigue test, the number of cycles in the air (without treated specimens) was (46427), whereas the number of cycles in solution was (33452); the specimens in solution had a lower fatigue resistance.
2) According to the results, the first layer of laser cladding was the foundation material, while the second layer was laser cladding.
3) Laser-clad specimens have a lower fatigue life than comparable-sized specimens without cladding.
4) Cladding of alloy st-52 with Inconel 600 alloy indicates bad fatigue results. Unconvincing results due to the decrease in fatigue and corrosion fatigue resistances after Inconel 600 alloy cladding. The number of cycles for fatigue failure with cladding in the air was (55774), and the number of cycles for corrosion fatigue with cladding was (24450).

Author contribution

All authors contributed equally to this work.

Funding

This research received no specific grant from any funding agency in the public, commercial, or not-for-profit sectors.

Data availability statement

The data that support the findings of this study are available on request from the corresponding author.

Conflicts of interest

The authors declare that there is no conflict of interest.

References

[1] Ganjali, M.2019. Recent Advances in the Design of Nanocomposite Materials via Laser Techniques for Biomedical Applications, pp.8.Adv Nanostructured Compos.

[2] M. Brandt, S. Sun, N. Alam, P. Bendeich, A. Bishop, Laser cladding repair of turbine blades in power plants: from research to commercialisation, Int. Heat. Treat. Surf. Eng., 3 (2009) 105–114. https://doi.org/10.1179/174951409X12542264513843

[3] W.-Z. Wang, F.-Z. Xuan, K.-L. Zhu, S.-T. Tu, Failure analysis of the final stage blade in steam turbine, Eng. Fail. Anal., 14 (2007) 632–641. https://doi.org/10.1016/j.engfailanal.2006.03.004

[4] R. K. Bhamu, A. Shukla, S. C. Sharma, S. P. Harsha, Low-Cycle Fatigue Life Prediction of LP Steam Turbine Blade for Various Blade–Rotor Fixity Conditions, J. Fail. Anal. Preven., 21(2021) 2256–2277. https://doi.org/10.1007/s11668-021-01282-9

[5] S. Prifiharni, H. Perdana, T. B. Romijarso, B. Adjiantoro, A. Juniarsih, E. Mabruri, The hardness and microstructure of the modified 13Cr steam turbine blade steel in tempered conditions, Int. J. Eng. Technol., 8 (2017) 2672–2675. https://doi.org/10.21817/ijet/2016/v8i6/160806224

[6] Valente, C., Morgado, T., Sharma, N. 2020. LASER cladding—a post processing technique for coating, repair and re-manufacturing, In: Gupta, K. (eds) Materials Forming, Machining and Post Processing. Materials Forming, Machining and Tribology, pp 231–249 .Springer, Cham.. https://doi.org/10.1007/978-3-030-18854-2_10

[7] J. Yao, Q. Zhang, F. Kong, Q. Ding, Laser hardening techniques on steam turbine blade and application, Phys Procedia, 5 (2010) 399–406. https://doi.org/10.1016/j.phpro.2010.08.161

[8] M. Katinić, D. Kozak, I. Gelo, D. Damjanović, Corrosion fatigue failure of steam turbine moving blades: A case study, Eng. Fail. Anal., 106 (2019) 104136. https://doi.org/10.1016/j.engfailanal.2019.08.002

[9] M. Nurbanasari, Crack of a first stage blade in a steam turbine, Case Stud. Eng. Fail. Anal., 2 (2014) 54–60. https://doi.org/10.1016/j.csefa.2014.04.002

[10] Khalifeh, A. Stress corrosion cracking damages, in Failure analysis, 2019. https://doi.org/10.5772/intechopen.80826

[11] R. Ebara, Corrosion fatigue crack initiation behavior of stainless steels, Procedia Eng., 2 (2010) 1297–1306. https://doi.org/10.1016/j.proeng.2010.03.141

[12] S.-X. Li , R. Akid, Corrosion fatigue life prediction of a steel shaft material in seawater, Eng. Fail. Anal., 34 (2013) 324–334. https://doi.org/10.1016/j.engfailanal.2013.08.004

[13] D. H. Abdeen, M. El Hachach, M. Koc, M. A. Atieh, A review on the corrosion behaviour of nanocoatings on metallic substrates, Materials , 12 (2019) 210. https://doi.org/10.3390/ma12020210

[14] P. Nguyen-Tri, T. A. Nguyen, P. Carriere, C. Ngo Xuan, Nanocomposite coatings: preparation, characterization, properties, and applications, Int. J. Corros., 2018 (2018)19. https://doi.org/10.1155/2018/4749501

[15] R. S. A. Hameed, A.-A. H. Abu-Nawwas, H. A. Shehata, Nano-composite as corrosion inhibitors for steel alloys in different corrosive media, Adv. Appl .Sci. Res., 4 (2013)126–129.

[16] G. Wang, Nanotechnology: The new features, arXiv Prepr arXiv181204939, 2018. https://doi.org/10.48550/arXiv.1812.04939

[17] L. K. Bhagi, P. Gupta, V. Rastogi, A brief review on failure of turbine blades,Proc STME-2013 Smart Technol Mech Eng Delhi, 2013. https://doi.org/10.13140/RG.2.1.4351.3768

[18] Vanderlinde, W. Energy dispersive X-ray analysis, Microelectron Fialure Anal Desk Ref, 434, 2019.

[19] Z. A. Abdulwahab, S. A. Ajeel, S. I. Jafar, Influence Of Laser Cladding on Behavior of Fatigue and Fatigue Corrosion, IOP Conf. Ser. Earth Environ. Sci, .961, 2022, 12035. https://doi.org/10.1088/1755-1315/961/1/012035

[20] A. Nair , A. Khan, Studies on effect of laser processed stellite 6 material and its electrochemical behavior, Optik , 220 (2020) 165221. https://doi.org/10.1016/j.ijleo.2020.165221

[21] O. A. Soylu, Determination of relationship between weld quality and mechanical strength in different steels. Middle East Technical University, 2004.

[22] D. Radaj, State□of□the□art review on extended stress intensity factor concepts, Fatigue Fract. Eng. Mater. Struct., 37(2014) 1–28. https://doi.org/10.1111/ffe.12120

[23] K. F. Walker, J. M. Lourenço, S. Sun, M. Brandt, C. H. Wang, Quantitative fractography and modelling of fatigue crack propagation in high strength AerMet® 100 steel repaired with a laser cladding process, Int .J. Fatigue, 94 (2017) 288–301. https://doi.org/10.1016/j.ijfatigue.2016.06.031